

# Structural Transformations and Magnetic Effects Induced by Solvent Exchange in the Spin Crossover Complex $[\text{Fe}(\text{bpp})_2][\text{Cr}(\text{bpy})(\text{ox})_2]_2$

Mari Carmen Giménez-López,<sup>[a]</sup> Miguel Clemente-León,<sup>[a]</sup> Eugenio Coronado,<sup>\*[a]</sup> Francisco M. Romero,<sup>\*[a]</sup> Sergiu Shova,<sup>[b][‡]</sup> and Jean-Pierre Tuchagues<sup>[b]</sup>

**Keywords:** Spin crossover / Iron / Solvent sensing / Hydration / Magnetic properties

Structural, thermal, magnetic and solvent-exchange properties of the spin crossover compound  $[\text{Fe}(\text{bpp})_2][\text{Cr}(\text{bpy})(\text{ox})_2]_2$  containing paramagnetic anions are given. This complex salt **1** crystallises as a dihydrate with two inequivalent (high-spin and low-spin)  $\text{Fe}^{\text{II}}$  sites. The dehydrated compound is a spin-crossover material with  $T_{1/2} \uparrow = 369 \text{ K}$  and  $T_{1/2} \downarrow = 353 \text{ K}$ . Rehydration takes place without loss of crystallinity, yielding

a polymorph (**2**) with 100 % high-spin  $\text{Fe}^{\text{II}}$  sites. The different high-spin fractions in **1** and **2** have been correlated to structural changes in the  $\text{Fe}^{\text{II}}$  second coordination sphere. The magnetic response to the presence of different sorbed molecules has also been explored.

(© Wiley-VCH Verlag GmbH & Co. KGaA, 69451 Weinheim, Germany, 2005)

The spin crossover between the diamagnetic low-spin (LS,  $S = 0$ ) and the paramagnetic high-spin (HS,  $S = 2$ ) states in iron(II) complexes has attracted much interest.<sup>[1]</sup> Although the purely molecular origin of the effect is clearly established by its observation in solution, cooperativity plays a key role in the solid state, where the phenomenon may be accompanied by a structural phase transition. The transition is triggered by a given external perturbation (light irradiation, pressure or temperature change) and the response (change of the optical and magnetic properties) may be observed abruptly with a hysteretic behaviour. These materials can then be considered as bistable systems suitable for practical applications.

In the search of increasing cooperativity, high-dimensional structures have been designed in which the functional molecular units are linked by bridging ligands.<sup>[2]</sup> Using this strategy, some nanoporous frameworks displaying spin crossover effects that are influenced by the reversible exchange of solvate molecules have been obtained.<sup>[3]</sup> Another approach relies on hydrogen bonding. In this context, the abrupt and hysteretic spin transitions of  $[\text{Fe}(\text{bpp})_2]\text{X}_2$  complex salts [bpp = 2,6-bis(pyrazol-3-yl)pyridine; X = anion] are well documented.<sup>[4]</sup> The amino groups of the pyrazolyl moieties can set up hydrogen bonds with its environment and this gives rise to a cooperative behaviour and a marked

dependence of the spin transition on the nature of the anion and the extent of hydration.<sup>[5]</sup> This family of compounds may provide good candidates for the study of solvation effects in spin crossover that can lead to interesting applications in molecular sensing. Further, these salts exhibit Light-Induced Excited Spin State Trapping (LIESST) effects at high temperatures with relatively long lifetimes of the photoinduced metastable states.<sup>[6]</sup> In this report, we give evidence for the strong dependence of the electronic configuration of the  $\text{Fe}^{2+}$  cations on the exchange of guest solvent molecules in the salt  $[\text{Fe}(\text{bpp})_2][\text{Cr}(\text{bpy})(\text{ox})_2]_2$  (**1**) (bpy = 2,2'-bipyridine; ox = oxalate dianion). The complex anion has been chosen for its ability to form hydrogen bonds and  $\pi$ - $\pi$  stacking interactions.<sup>[7]</sup>

Compound **1** crystallises as a dihydrate  $[\text{Fe}(\text{bpp})_2][\text{Cr}(\text{bpy})(\text{ox})_2]_2 \cdot 2\text{H}_2\text{O}$  and its structure<sup>[8]</sup> comprises isolated  $[\text{Fe}(\text{bpp})_2]^{2+}$  and  $[\text{Cr}(\text{bpy})(\text{ox})_2]^-$  complexes and water molecules. Two crystallographically independent octahedral iron(II) sites, Fe(1A) and Fe(1B), were found (Figure 1a). Both sites have a pseudo  $C_{2v}$  symmetry, with the tridentate bpp ligand binding to the iron ion in meridional positions. The Fe(1A) coordination sphere is consistent with high-spin  $\text{Fe}^{\text{II}}$ , with Fe–N bond lengths lying in the range 2.146(2)–2.210(2) Å. In contrast, the Fe–N bond lengths of the Fe(1B) site are typical low-spin values, lying in the range 1.921(2)–1.976(2) Å. Several examples of coexistence of HS and LS species in the same compound have been reported. In these cases, the different iron centres adopt similar ligand-binding geometries but different second coordination spheres.<sup>[9]</sup> We observed a similar behaviour: the four non-coordinating N–H groups of complex **A** (Figure 1a) are hydrogen-bonded to three  $[\text{Cr}(\text{bpy})(\text{ox})_2]^-$  anions and one water molecule, whereas complex **B** is connected to four  $[\text{Cr}(\text{bpy})(\text{ox})_2]^-$  anions. Since the oxalate oxygen atom of the

[a] Institut de Ciència Molecular, Universitat de València  
Dr. Moliner, 50, 46100 Burjassot, Spain  
Fax: +34-963-544-859  
E-mail: fmrm@uv.es

[b] Laboratoire de Chimie de Coordination du CNRS  
205 route de Narbonne. 31077 Toulouse cedex, France  
Fax: +33-5-61553003  
E-mail: tuchague@lcc-toulouse.fr

[‡] On leave from: State University of Moldova,  
Mateevici str. 60, 2009 Chisinau, Moldova

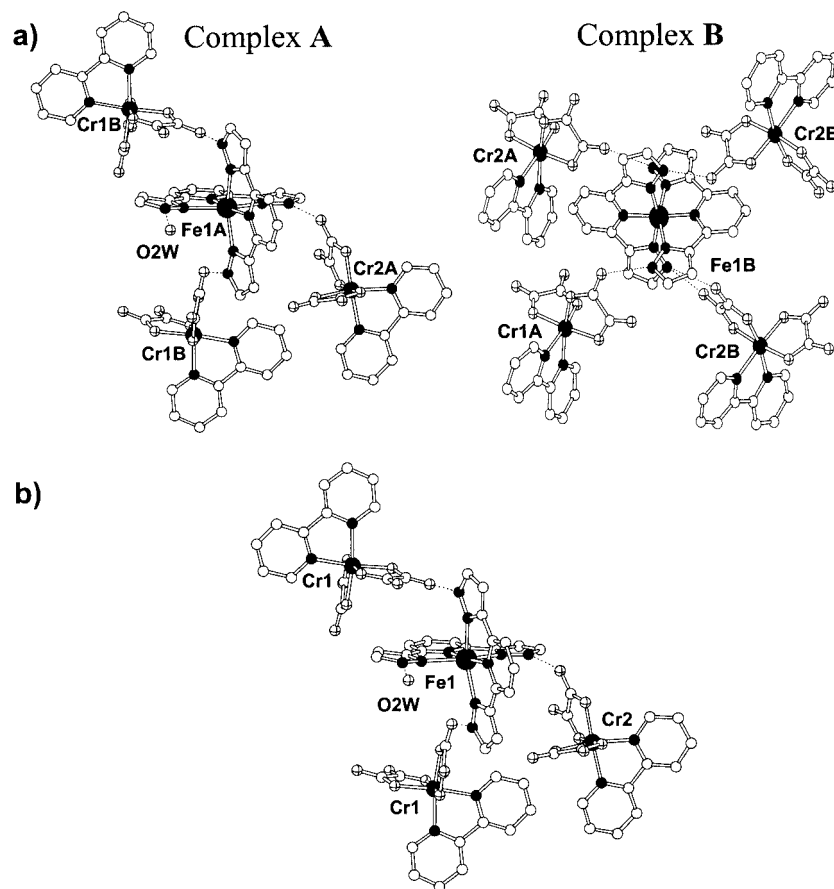


Figure 1. View of the crystal structure of the hydrated salt  $[\text{Fe}(\text{bpp})_2][\text{Cr}(\text{bpy})(\text{ox})_2]_2 \cdot 2\text{H}_2\text{O}$  showing the first and second coordination spheres of the  $\text{Fe}^{2+}$  cations; a) original sample (1), b) rehydrated sample (2).

anion is a better hydrogen-bonding acceptor than water, the electron density of the non-coordinating nitrogen atoms of **B** is increased with respect to **A**. This leads to stronger donor–metal  $\sigma$ -interaction, favouring the LS state for complex **B**.

The magnetic properties of **1** are in agreement with this structural analysis. The product of the molar magnetic susceptibility with the temperature,  $\chi_M T$ , (Figure 2, curve 1) shows a nearly constant value of  $5.5 \text{ emu} \cdot \text{K} \cdot \text{mol}^{-1}$  from 50 K to room temperature, in agreement with the presence of half of the  $\text{Fe}^{2+}$  ions in the HS state and two  $\text{Cr}^{3+}$  ions per formula unit. At temperatures above 320 K,  $\chi_M T$  decreases and reaches a minimum at 356 K, followed by an increase to a value of  $7 \text{ emu} \cdot \text{K} \cdot \text{mol}^{-1}$  at 400 K, indicating that 100% of the Fe sites are HS at this temperature. On cooling now the compound (curve 2) below 300 K, a  $\chi_M T$  value of  $3.7 \text{ emu} \cdot \text{K} \cdot \text{mol}^{-1}$  is observed, as expected for two uncorrelated  $\text{Cr}^{3+}$  ions with all the iron(II) centres in the LS configuration. Successive temperature cycles (heating and cooling modes, Figure 2) reveal that the preheated sample displays a spin crossover behaviour with  $T_{1/2} \uparrow = 369 \text{ K}$  and  $T_{1/2} \downarrow = 353 \text{ K}$ .

The thermogravimetric analysis (TGA) of **1** (Figure 3a) indicates a weight loss of about 3% upon heating of the compound in the 300–380 K range. This is clearly a dehy-

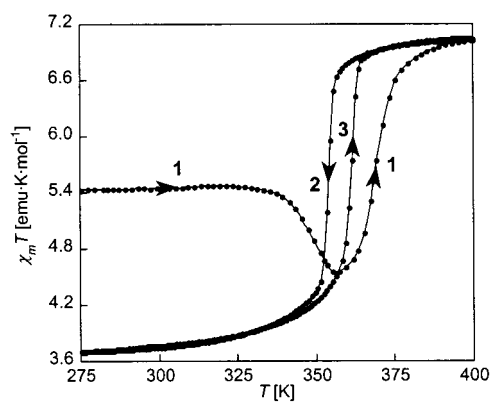


Figure 2. Temperature dependence of  $\chi_M T$  for compound **1** in the 275–400 K range. Curve 1: original sample in the heating mode. Curves 2 and 3: subsequent temperature cycle (cooling and heating modes, respectively).

dration process that corresponds to the loss of two water molecules. The DSC measurement of the original sample (Figure 3b, curve 1) shows two different endothermic processes that can be attributed to dehydration. In the cooling mode (curve 2), the dried sample exhibits an exothermic feature at 354 K, characteristic of a high-spin to low-spin transition. This process was masked in the measurement of

the original hydrated sample and it can be also characterised by the sharp endothermic peak observed in the heating mode (curve 3) at 358 K.

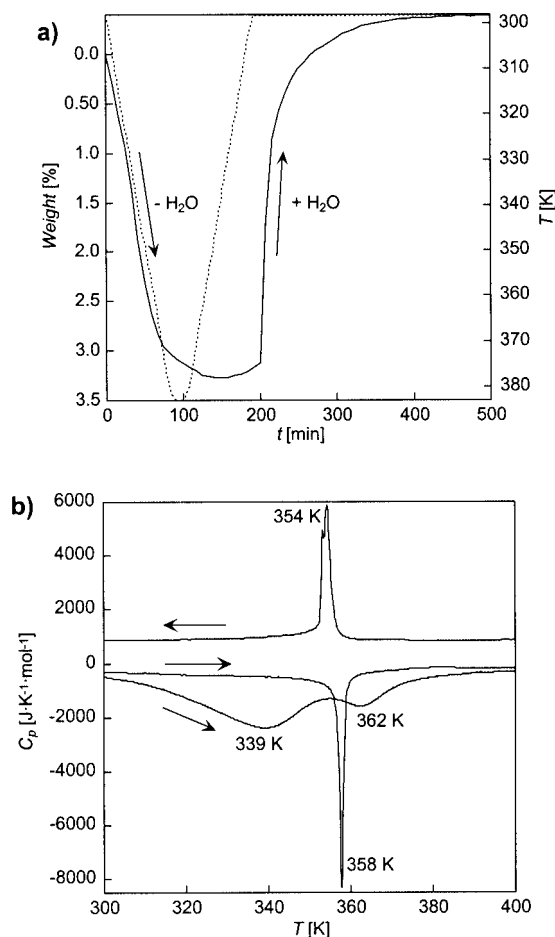


Figure 3. a) Thermogravimetric analysis of compound **1** showing the dehydration-rehydration process. The weight loss of the sample was measured in the 300–380 K range at a constant heating rate of 1 K/min. Then the sample was allowed to cool in an ambient atmosphere. b) Differential scanning calorimetry of **1** in the range of 300–400 K. Curve 1: original sample in the heating mode. Curves 2 and 3: subsequent temperature cycle (cooling and heating modes, respectively).

Based on the thermal and magnetic studies, it is possible to conclude that the initial sweeping-rate-dependent decrease of  $\chi_M T$  is due to a change of spin accompanying the dehydration, while the abrupt increase/decrease of  $\chi_M T$  observed at higher temperatures is associated to a spin transition of the dehydrated compound. This behaviour is typical of  $[\text{Fe}(\text{bpp})_2]\text{X}_2$  salts.<sup>[9]</sup> The main difference here is that the spin transition is pushed to very high temperatures as compared to previous examples. Removal of water molecules may allow a fourth  $[\text{Cr}(\text{bpy})(\text{ox})_2]^-$  anion to be located in the second coordination sphere of Fe(1A), giving rise to a strong stabilisation of the LS state.

Rehydration of a dried sample of **1** proceeds readily and the total weight of the original sample can be recovered in a few minutes (Figure 3a). Surprisingly, the rehydrated sam-

ple and the original sample show different magnetic behaviours. Below 50 K, both samples exhibit a continuous increase of  $\chi_M T$  with increasing temperature. This can be attributed to zero-field splitting and spin-orbit coupling effects, although intermolecular interactions between the different spin carriers cannot be discarded. From 50 K to room temperature (Figure 4a), the  $\chi_M T$  value of the rehydrated sample is equal to  $7.5 \text{ emu}\cdot\text{K}\cdot\text{mol}^{-1}$ , suggesting that all the  $\text{Fe}^{2+}$  cations are in the HS state. As shown for the original sample, loss of water causes a sudden decrease of  $\chi_M T$  above room temperature. By further heating, the spin transition characteristic of the dehydrated sample is again observed. TGA and DSC studies confirm again the hypotheses based on the magnetic behaviour. The markedly different magnetic properties of the original and rehydrated samples are very interesting: the magnetic measurements reflect the history of the dehydration-rehydration process.

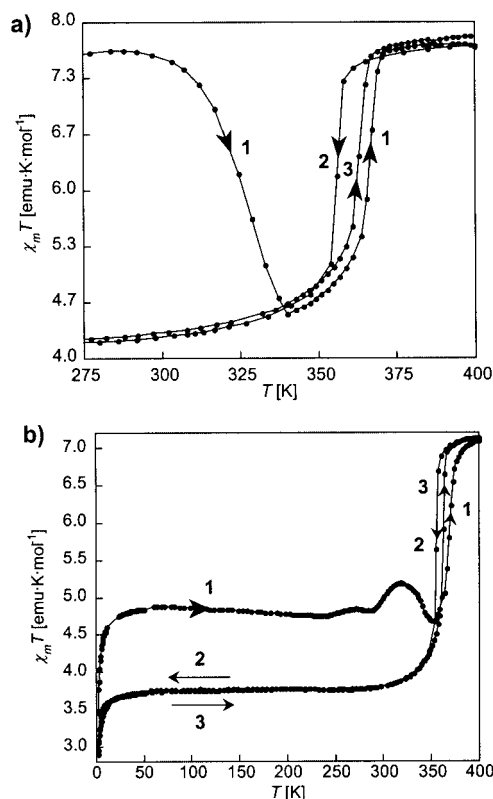


Figure 4. Temperature dependence of  $\chi_M T$  for rehydrated (a) and MeOH-solvated (b) samples in the 2–400 K range. Curves 1: first treatment in the heating mode. Curves 2 and 3: subsequent temperature cycles (cooling and heating modes, respectively).

Temperature-dependent X-ray diffraction data suggest that this process occurs without drastic changes in the crystal structure. This prompted us to study the crystal structure of the rehydrated phase. For this purpose, a single crystal of **1** was heated to 343 K under dry nitrogen until constant loss of weight in a TGA instrument. Afterwards, the crystal was kept in ambient atmosphere to allow rehydration and the structure of the rehydrated single crystal

was solved by X-ray diffraction measurements (Figure 1b). The resulting compound **2** is also a dihydrate and it retains the same crystal symmetry.<sup>[10]</sup> One of the unit cell parameters is halved and only one independent Fe<sup>II</sup> site is now present. Its environment is very similar to that observed for the HS site Fe(1A) of the original compound, with Fe–N bond lengths in the 2.145(3)–2.204(3) Å range and the second coordination sphere containing three [Cr(bpy)(ox)<sub>2</sub>]<sup>–</sup> anions and one water molecule hydrogen-bonded to the pyrazolyl moieties. Hence, after rehydration the two crystallographically independent high-spin Fe(1A) and low-spin Fe(1B) sites become equivalent and a 100% content of HS species is observed.

These findings suggest that spin crossover materials can be very sensitive to exchangeable guest solvent molecules such as alcohols, which are able to form hydrogen bonds. In principle, it could be possible to correlate the nature of the absorbed solvent with the magnetic properties; in such a way that spin crossover could be used as a molecular probe. As an example, **1** has been dehydrated and resolvated with methanol. The solvation process can be easily monitored in a TGA apparatus. An increase of weight corresponding to the absorption of one MeOH molecule was observed. Magnetic measurements of this methanol-solvated sample (Figure 4b) show a distinct behaviour with respect to the rehydrated material. The  $\chi_M T$  value at 200 K is 4.8 emu·K·mol<sup>–1</sup> and corresponds to 33% Fe<sup>II</sup> centres in the HS state. This value remains nearly constant on increasing the temperature. At 330 K, desolvation starts and  $\chi_M T$  decreases to a minimum value at 350 K.<sup>[11]</sup> Further heating results in a sudden increase of the magnetic signal that corresponds to the spin transition of the desolvated sample. Successive temperature cycles reveal the same magnetic behaviour than that observed for the dehydrated material.

To summarize, the dry material at room temperature exhibits only the paramagnetism of the Cr<sup>III</sup> centres, with all the Fe<sup>2+</sup> ions in their LS configuration. Upon exposure to ambient moisture, the compound undergoes a spin crossover to an HS phase. This transition can be correlated to the replacement of a [Cr(bpy)(ox)<sub>2</sub>]<sup>–</sup> anion by a water molecule in the second coordination sphere of the Fe<sup>2+</sup> cations. In contrast, treatment of a dry sample with dry methanol vapours yields a material with only 33% of the Fe<sup>II</sup> sites in the HS configuration.

Clearly, the magnetic properties of this spin crossover compound are very sensitive to the presence of different solvates. This is a well-known effect that has recently drawn special attention in the field of crystal engineering.<sup>[12]</sup> However, there are only a few qualitative studies on the influence of absorption of solvent molecules in the spin states of dry compounds.<sup>[13]</sup> These studies lack of any structural evidence. The present work provides a deeper insight into the spin changes associated with different resolution processes. As compared to previously reported examples based on high-dimensional networks, our approach relies simply on hydrogen bonding. Further work will be devoted to study the influence of the paramagnetic anion on the solvent sensing properties.

## Experimental Section

**General:** All chemicals and solvents were used as received. Ba[Cr(bpy)(ox)<sub>2</sub>]<sub>2</sub>·3H<sub>2</sub>O and bpp were synthesized according to previously described methods.<sup>[14,15]</sup>

**[Fe(bpp)<sub>2</sub>][Cr(bpy)(ox)<sub>2</sub>]<sub>2</sub>·2H<sub>2</sub>O (**1**):** A solution of bpp (140 mg, 0.66 mmol) and FeSO<sub>4</sub>·7H<sub>2</sub>O (92 mg, 0.33 mmol) in 40 mL of MeOH was added to a suspension of Ba[Cr(bpy)(ox)<sub>2</sub>]<sub>2</sub>·3H<sub>2</sub>O (361 mg, 0.33 mmol) in 30 mL of water. The resulting mixture was stirred for 2 h to promote complete precipitation of BaSO<sub>4</sub>, which was removed by filtration. After a few days, large red crystals were obtained by slow concentration of the mother liquor. Yield: 199 mg (53%). IR (KBr):  $\tilde{\nu}$  = 3544 (w), 3444 (w), 3127 (m), 2921 (m), 1711 (vs), 1679 (vs), 1653 (vs), 1609 (s), 1370 (s), 803 (m), 773 (m), 543 (m), 415 (w) cm<sup>–1</sup>. C<sub>50</sub>H<sub>38</sub>Cr<sub>2</sub>FeN<sub>14</sub>O<sub>18</sub> (1282.8): calcd. C 46.82, H 2.99, N 15.29; found C 46.82, H 2.93, N 15.08; calcd. Cr/Fe 66.6:33.3, found 65.8/34.2.

**Physical Measurements:** Dc magnetic susceptibility measurements were performed on polycrystalline samples using a magnetometer (Quantum Design MPMS-XL-5) equipped with a SQUID sensor. Variable-temperature measurements were carried out in the temperature range 2–400 K in a magnetic field of 0.1 T. The temperature sweeping rate was the same for the experiments performed on the original and methanol-solvated samples: 0.5 K·min<sup>–1</sup> (2–10 K), 1 K·min<sup>–1</sup> (10–50 K), 5 K·min<sup>–1</sup> (50–200 K), 2 K·min<sup>–1</sup> (200–400 K). For the rehydrated sample, the last change in the sweeping rate was set to 340 K. Thermogravimetric measurements were carried out with a Mettler Toledo TGA/SDTA 851 apparatus in the 298–1373 K temperature range under nitrogen and at a scan rate of 5 K·min<sup>–1</sup>. The dehydration-rehydration process was monitored by heating the ground sample under a stream of nitrogen from 298 to 383 K (1 K·min<sup>–1</sup>). Then, the system was kept at this temperature during 20 min to allow complete loss of water molecules. Afterwards, the sample was cooled to 298 K. At this point, the stream of nitrogen was replaced by a stream of humid air to allow complete rehydration of the sample. For the solvation experiment, a stream of nitrogen saturated with dry methanol was used. The total flux of nitrogen was constant during the experiments. After saturation (constant weight), the samples were quickly introduced in the SQUID apparatus, protecting them from the environment. Heat capacity measurements under nitrogen were performed in a Mettler Toledo DSC 821e apparatus with warming and cooling rates equal to 4 K·min<sup>–1</sup> from 253 to 423 K. IR transmission measurements of KBr pellets were recorded at room temperature with a Nicolet Avatar 320 FT-IR spectrophotometer in the range 4000–400 cm<sup>–1</sup>. C,H,N elemental analyses were carried out in a CE instruments EA 1110 CHNS analyzer. The Cr/Fe ratios were measured with a Philips ESEM X230 scanning electron microscope equipped with an EDAX DX-4 microsonde.

- [1] "Spin Crossover in Transition Metal Compounds I–III", in: *Topics in Current Chemistry* (Eds.: P. Güttlich, H. A. Goodwin), **2004**, pp. 233–235, and references therein.
- [2] a) J. A. Real, E. Andrés, M. C. Muñoz, M. Julve, T. Granier, A. Bousseksou, F. Varret, *Science* **1995**, *268*, 265; b) V. Niel, A. L. Thompson, M. C. Muñoz, A. Galet, A. E. Goeta, J. A. Real, *Angew. Chem. Int. Ed.* **2003**, *42*, 3759; c) A. Galet, V. Niel, M. C. Muñoz, J. A. Real, *J. Am. Chem. Soc.* **2003**, *125*, 14224; d) V. Niel, M. C. Muñoz, A. B. Gaspar, A. Galet, G. Levchenko, J. A. Real, *Chem. Eur. J.* **2002**, *8*, 2446.
- [3] G. J. Halder, C. J. Kepert, B. Moubaraki, K. S. Murray, J. D. Cashion, *Science* **2002**, *298*, 1762.
- [4] a) K. H. Sugiyarto, H. A. Goodwin, *Aust. J. Chem.* **1988**, *41*, 1645; b) H. Sugiyarto, K. Weitzner, D. C. Craig, H. A. Good-

- win, *Aust. J. Chem.* **1997**, *50*, 869; c) K. H. Sugiyarto, W. A. McHale, D. C. Craig, D. Rae, M. L. Scudder, H. A. Goodwin, *Dalton Trans.* **2003**, 2443.
- [5] K. H. Sugiyarto, D. C. Craig, A. D. Rae, H. A. Goodwin, *Aust. J. Chem.* **1994**, *47*, 869.
- [6] a) Th. Buchen, P. Gütllich, K. H. Sugiyarto, H. A. Goodwin, *Chem. Eur. J.* **1996**, *2*, 1134; b) S. Marcen, L. Lecren, L. Capes, H. A. Goodwin, J. F. Létard, *Chem. Phys. Lett.* **2002**, *358*, 87.
- [7] M. C. Muñoz, M. Julve, F. Lloret, J. Faus, M. Andruh, *J. Chem. Soc., Dalton Trans.* **1998**, 3125.
- [8] Crystal data for **1**:  $\text{C}_{100}\text{H}_{76}\text{Cr}_4\text{Fe}_2\text{N}_{28}\text{O}_{36}$ ,  $M = 2565.59$ , crystal dimensions:  $0.50 \times 0.45 \times 0.05$  mm, triclinic,  $P\bar{1}$ ,  $a = 15.5434(15)$ ,  $b = 17.723(2)$ ,  $c = 20.985(2)$  Å,  $\alpha = 102.002(12)$ ,  $\beta = 103.291(11)$ ,  $\gamma = 103.299(12)$ ,  $V = 5263.4(9)$  Å<sup>3</sup>,  $Z = 2$ ,  $\rho_{\text{calcd.}} = 1.629$  Mg m<sup>-3</sup>,  $\mu(\text{Mo-K}\alpha) = 0.769$  mm<sup>-1</sup>. A dark-red plate-like single crystal of **1** was used for data collection at 180 K with a Stoe Imaging Plate Diffractometer System (IPDS) diffractometer equipped with a graphite-monochromated Mo- $K\alpha$  radiation source ( $\lambda = 0.71073$  Å), and an Oxford Cryostream Cooler Device. Data were collected using the  $\phi$  rotation movement with a crystal-to-detector distance of 70 mm ( $\phi = 0.0$ – $250^\circ$ ,  $\Delta\phi = 1.4^\circ$ ). Of 52754 measured reflections, 19375 ( $4.14^\circ < 2\theta < 52.20^\circ$ ) were independent ( $R_{\text{int}} = 0.0470$ ) and used to refine 1812 parameters. Semiempirical absorption corrections were made based on equivalent reflections with the program MULTISCAN.<sup>[16]</sup> The structure was solved by direct methods using SHELXS-97<sup>[17]</sup> and refined by full-matrix least squares on  $F_o^2$  with SHELXL-97<sup>[18]</sup> with anisotropic displacement parameters for non-hydrogen atoms. All H atoms attached to carbon atoms were introduced in idealized positions ( $d_{\text{CH}} = 0.96$  Å) using the riding model with their isotropic displacement parameters fixed at 120% of their riding atom. Positional parameters of the hydrogen atoms of three solvate water molecules were obtained from difference Fourier syntheses and verified by the geometric parameters of hydrogen bonds. O(4w) molecules, which are positioned in hydrophobic cavities, are disordered among two positions with a 0.6:0.4 ratio of the occupancy factors. There are no short intermolecular contacts from O(4w) which can be characterized as possible H-bonds. The hydrogen atoms for this water molecule were not localized. There is only one short intermolecular contact  $[\text{O}4\text{w} \cdots \text{O}(2\text{B}) = 2.826$  Å], which can be characterized as possible H-bond.  $R_1 = 0.0419$  for 14420 reflections with  $I \geq 2\sigma(I)$ ,  $wR_2 = 0.1071$ ;  $R_1 = 0.0623$ ,  $wR_2 = 0.1194$ ,  $\text{GOF} = 0.984$  for all data. Max./min. residual peaks in the final difference map:  $0.955/-0.482$  e<sup>-</sup>Å<sup>-3</sup>. CCDC-258048 contains the supplementary crystallographic data for this paper. These data can be obtained free of charge from The Cambridge Crystallographic Data Centre via [www.ccdc.cam.ac.uk/data\\_request/cif](http://www.ccdc.cam.ac.uk/data_request/cif).
- [9] K. H. Sugiyarto, M. L. Scudder, D. C. Craig, H. A. Goodwin, *Aust. J. Chem.* **2000**, *53*, 755.
- [10] Crystal data for **2**:  $\text{C}_{50}\text{H}_{38}\text{Cr}_2\text{FeN}_{14}\text{O}_{18}$ ,  $M = 1282.79$ , crystal dimensions:  $0.20 \times 0.12 \times 0.05$  mm, triclinic,  $P\bar{1}$ ,  $a = 9.04700(10)$ ,  $b = 15.6410(2)$ ,  $c = 20.6980(3)$  Å,  $\alpha = 102.5530(5)$ ,  $\beta = 102.0710(5)$ ,  $\gamma = 103.9340(5)$ ,  $V = 2666.95(6)$  Å<sup>3</sup>,  $Z = 2$ ,  $\rho_{\text{calcd.}} = 1.597$  Mg m<sup>-3</sup>,  $\mu(\text{Mo-K}\alpha) = 0.758$  mm<sup>-1</sup>. A dark-red plate-like single crystal of **2** was used for data collection with a Nonius Kappa CCD diffractometer ( $4.34^\circ < 2\theta < 55.32^\circ$ ) equipped with a graphite-monochromated Mo- $K\alpha$  radiation source ( $\lambda = 0.71073$  Å). Data collection was performed at 180 K. Of 22949 measured reflections, 12198 were independent ( $R_{\text{int}} = 0.0403$ ) and used to refine 793 parameters. The structure was solved by direct methods (SIR97)<sup>[19]</sup> and refined against  $F^2$  with a full-matrix least-squares algorithm using SHELXL-97<sup>[18]</sup> and the WinGX (1.64) software package.<sup>[20]</sup> All non-hydrogen atoms were refined anisotropically. H-atoms were added in calculated positions and refined riding on the corresponding atoms except H atoms of –NH groups and water molecules. H-atoms of –NH groups were located by difference Fourier maps and refined isotropically. H-atoms of water molecules were calculated on the basis of geometry and force-field considerations using the CALC-OH program<sup>[21]</sup> and refined isotropically fixing the H–H and H–O distances. Final  $R [I > 2\sigma(I)]$ :  $R_1 = 0.0538$ ,  $wR_2 = 0.1505$ ; final  $R$  (all data):  $R_1 = 0.0933$ ,  $wR_2 = 0.1961$ . Max./min. residual peaks in the final difference map:  $0.700/-1.230$  e<sup>-</sup>Å<sup>-3</sup>. CCDC-259006 contains the supplementary crystallographic data for this paper. These data can be obtained free of charge from The Cambridge Crystallographic Data Centre via [www.ccdc.cam.ac.uk/data\\_request/cif](http://www.ccdc.cam.ac.uk/data_request/cif).
- [11] Between 300 and 330 K, a slight increase of the magnetic signal is observed. This behaviour is also observed in a blank measurement performed with a sample dehydrated in the TGA equipment and then transferred to the SQUID instrument. Besides this accident, the magnetic behaviour of this sample is the same as that observed in curves 2 and 3 for dry samples. This accident is most probably due to the presence of humidity within the equipment.
- [12] M. Hostettler, K. W. Törnroos, D. Chernyskov, B. Vangdal, H. B. Bürgi, *Angew. Chem. Int. Ed.* **2004**, *43*, 4589.
- [13] a) Y. Garcia, P. J. van Koningsbruggen, E. Codjovi, R. Lapouyade, O. Kahn, L. Rabardel, *J. Mater. Chem.* **1997**, *7*, 857; b) Y. Garcia, P. J. van Koningsbruggen, R. Lapouyade, L. Fournès, L. Rabardel, O. Kahn, V. Ksenofontov, G. Levchenko, P. Gütllich, *Chem. Mater.* **1998**, *10*, 2426; c) O. Roubeau, J. G. Haasnoot, E. Codjovi, F. Varret, J. Reedijk, *Chem. Mater.* **2002**, *14*, 2559.
- [14] J. A. Broomhead, *Aust. J. Chem.* **1962**, *15*, 228.
- [15] Y. Lin, S. A. Lang, *J. Heterocycl. Chem.* **1977**, *14*, 345.
- [16] R. H. Blessing, *Acta Crystallogr. A* **1995**, *51*, 33.
- [17] G. M. Sheldrick, *SHELXS-97, Program for Crystal Structure Solution*, University of Göttingen, Göttingen, Germany, **1990**.
- [18] G. M. Sheldrick, *SHELXL-97, Program for the refinement of crystal structures from diffraction data*, University of Göttingen, Göttingen, Germany, **1997**.
- [19] A. Altomare, M. C. Burla, M. Camalli, G. Casciarano, C. Giacovazzo, A. Guagliardi, A. G. G. Moliterni, G. Polidori, R. Spagna, *J. Appl. Crystallogr.* **1999**, *32*, 115.
- [20] L. J. Farrugia, *J. Appl. Crystallogr.* **1999**, *32*, 837.
- [21] M. Nardelli, *J. Appl. Crystallogr.* **1999**, *32*, 563.

Received March 17, 2005

Published Online: June 14, 2005